The Uniqueness of Human Vulnerability to Brain Aging in Great Ape Evolution

Sam Vickery[1,2], Kaustubh R. Patil[1,2], Robert Dahnke[3,4,5], William D. Hopkins[6], Chet C. Sherwood[7], Svenja Caspers[8,9,10], Simon B. Eickhoff[1,2], Felix Hoffstaedter[1,2]

[1] Institute of Systems Neuroscience, Medical Faculty & University Hospital Düsseldorf, Heinrich-Heine-University, Düsseldorf, Germany.

[2] Institute of Neuroscience and Medicine (INM-7) Research Centre Jülich, Jülich, Germany

[3] Structural Brain Mapping Group, Department of Neurology, Jena University Hospital, Jena, Germany

[4] Structural Brain Mapping Group, Department of Psychiatry and Psychotherapy, Jena University Hospital, Jena, Germany

[5] Center of Functionally Integrative Neuroscience, Department of Clinical Medicine, Aarhus University, Denmark

[6] Department of Comparative Medicine, Michale E Keeling Center for Comparative Medicine and Research, The University of Texas MD Anderson Cancer Center, Bastrop, Texas

[7] Department of Anthropology and Center for the Advanced Study of Human Paleobiology, The George Washington University, Washington, DC, USA.

[8] Institute of Neuroscience and Medicine (INM-1), Research Centre Jülich, Jülich, Germany

[9] Institute for Anatomy I, Medical Faculty & University Hospital Düsseldorf, Heinrich-Heine-University, Düsseldorf, Germany

[10] JARA-BRAIN, Jülich-Aachen Research Alliance, Jülich, Germany

Abstract

Aging is associated with stable decline in the brain's gray matter. This spatially specific, morphological change in humans has also recently been shown in chimpanzees. The correspondence between species-specific cortical expansion and the degree of brain structure deterioration in aging remains poorly understood. Here, we present a data-driven, cross-species comparative framework and apply it to explore the relationship between gray matter alterations with age and cross-species cerebral expansion in chimpanzees and humans. In humans, we found a positive relationship between cerebral aging and cortical expansion, whereas, in chimpanzees no such relationship was found between aging and cortical expansion. The greater aging and expansion effects in higher-order cognitive regions like the orbito-frontal cortex were observed to be unique to humans. This resembles the last-in, first out hypothesis for neurodevelopment on the evolutionary scale and may suggest a biological cost for recent evolutionary developments of human faculties.

Introduction

With age, pronounced alterations occur in morphology and organization of the human brain with a distinct spatial pattern resulting in part from cellular atrophy in later life[1,2]. These changes are part of the normal aging process, although they may be further accelerated in some people by age-mediated disorders such as Alzheimer's disease, Parkinson's disease, and other neurodegenerative conditions[3]. Furthering our understanding about specific neurobiological and possible evolutionary influences on these brain aging spatial patterns, may provide insight into the brain changes in healthy aging and possible diagnostic markers for clinical outcomes. Historically, comparative neuroscience has been an effective catalyst for important discoveries regarding principles of anatomy and functional specializations of the human brain[4]. With open and collaborative endeavors such as the National Chimpanzee Brain Resource (NCBR) and the PRIMatE Date Exchange (PRIME-DE)[5], along with improved methodologies and imaging technology, large scale comparative neuroanatomy has become more accessible to answer new questions[6].

Morphological gray matter (GM) changes during aging have recently been shown to be present in one of humans' closest extant primate relative, chimpanzees (*Pan troglodytes*)[7,8]. The age-related morphological changes observed in chimpanzees are similar but at a lower magnitude compared to humans[8]. For example, age-related volumetric reduction of overall hippocampus and frontal cortex size are not evident in chimpanzees, but occurs in humans that could be related to humans comparatively extended lifespan[9]. Cognitive decline is also present in chimpanzees, but appears not as prominent as in humans[10]. In this context, understanding GM alterations during brain aging in great ape evolution (e.g. which includes humans and chimpanzees, as well as bonobos, gorillas, and orangutans) may aid in explaining the spatial distribution of morphological changes due to healthy aging and disease.

The comparison of neuroanatomy and brain functions across primate species is commonly informed by analyzing homologous brain regions[6,11–13]. Classically, these regional homologies are defined by manually delineating brain partitions, based on macroanatomy, gene expression, connectivity, and/or cytoarchitectonic features. This approach rests on the assumption that similar anatomical features result in a common functional organization across species and thereby enable an informative and meaningful comparison. However, homologies can be debatable and therefore can be influenced by subjective biases which is minimizes through a data-driven approach. The homologous-centric approach has proven to be effective and informative, although utilizing a more data-driven approach could supplement these techniques by removing subjective biases while still capturing important cross-species differences and incorporating species-specific features in a data-centric manner.

Chimpanzees offer an ideal referential model to investigate evolutionary changes in the human lineage as they share a last common ancestor with humans approximately 6 - 8 million years ago[14]. Accordingly, chimpanzees and humans have many genomic similarities[15] as well as cerebral structural features in common[16–18]. Consequently, chimpanzees present a unique comparison to infer distinctive evolutionary adaptations of the human brain, keeping in mind that their neurobiology reflects their own species-specific evolutionary adaptations. The multitude of commonalities and recent evolutionary divergence allows a further understanding of changes associated with selection for human specific adaptations that occurred after the split from a common ancestor. Previous studies have shown that multimodal association cortices in humans are disproportionately larger than in non-human primates[11,19,20]. The higher expansion of certain areas through human evolution may relate to specific functions, important for modern human cognition. Specifically, the expanded human prefrontal cortex (PFC)[11] might be associated with self-control and executive functioning[21] and the larger precuneus[19] with visuospatial processing[22]. Furthermore, the vulnerability of frontal cortical areas to aging processes is hypothesized to be related to their late maturation[23]. This refers

to the "last in, first out hypothesis" and interestingly similarities have been shown between cortical development and cross-species expansion[24].

In this study, we directly compare age-mediated GM changes in chimpanzees and humans, which represent two species in the Hominidae family (i.e., great apes) and explore their relationship with cross-species cerebral expansion. For inter-species comparison, we developed a multivariate data-driven comparative framework that applies voxel-wise clustering based on GM variability within each species independently. The optimal low dimensional representation of brain morphology for each species is then employed in a cross-species investigation of aging and cortical expansion. Comparative data for calculating cross-species expansion was provided by relatively recent phylogenetic ancestors. Accordingly, humans were compared to chimpanzees and chimpanzees were compared to olive baboons (Papio anubis) and rhesus macaques (Macaca mulatta), two commonly researched cercopithecid monkey species. Therefore, we can ascertain whether such a relationship is unique to modern humans or instead might be a feature shared with chimpanzees that originated at the divergence of the great ape lineages from other primates.

To summarize, we present a novel technique for cross-species comparison of structural brain organization and demonstrate its utility by comparing the relationship between cerebral aging and cross-species expansion in humans and chimpanzees. Our data-driven approach uses both species-specific information in addition to cross-species similarity to create an interpretable low-dimensional brain parcellation for comparison. We show that the resulting parcellation aligns with known macroanatomical structures in humans and chimpanzees. Utilizing this comparative framework, we examine spatial differences in brain aging and cerebral expansion between the two great ape species. Finally, we present evidence for a relationship between local age-mediated GM changes and recent cortical expansion in humans that is not present in chimpanzees.

Results

Our cross-species comparative approach was based on structural magnetic resonance imaging (MRI) scans from 189 chimpanzees and 480 human brains (Fig. 1B). Orthogonal projective non-negative matrix factorization (OPNMF)[25,26] was applied to normalized GM maps within each species independently. The orthogonality and non-negativity constraints of OPNMF results in a spatially continuous, parts-based representation of the input data based on regional covariance of brain structure within each species[27]. OPNMF has been extensively used with human neuroimaging data yielding anatomically meaningful correspondence of clustering solutions[25,28–31].

The comparative framework utilizing OPNMF as well as the creation of the cross-species expansion maps is outlined in Figure 1A. The approach begins with separately segmenting and normalizing the individual chimpanzee and human images utilizing species-specific templates and pipelines[8,32]. The processed GM maps for each species are parcellated independently using OPNMF over a range of granularities (2-40) and bootstrapped to ensure stability of the solutions accuracy. The bootstrapped solution accuracy measure assessed using the reconstruction error (RE) is used in part, to select the optimal number of parcels for cross-species comparison. For direct cross-species comparison, the JunaChimp average chimpanzee T1-weighted (T1w) template[8] is applied to the human preprocessing pipeline to create a representative chimpanzee to human deformation field map. This represents the non-linear deformations required to map morphological macroanatomical

features of the JunaChimp[8] template brain to the standard ICBM 2009c Nonlinear Asymmetric human template[33]. The chimpanzee to human deformation map is used to non-linearly register the chimpanzee OPNMF solutions to the human template space for the analysis of parcel or factor similarity using the adjusted rand index (ARI). This cross-species parcel similarity of multivariate GM morphology are used for the selection of optimal parcellation granularity, together with species-specific OPNMF reconstruction error change (see *Comparative Brain Parcellations* for more information). To create cross-species expansion maps, average population templates from three non-human primate species were processed, chimpanzee[8], olive baboon[34], and rhesus macaque[35–37].

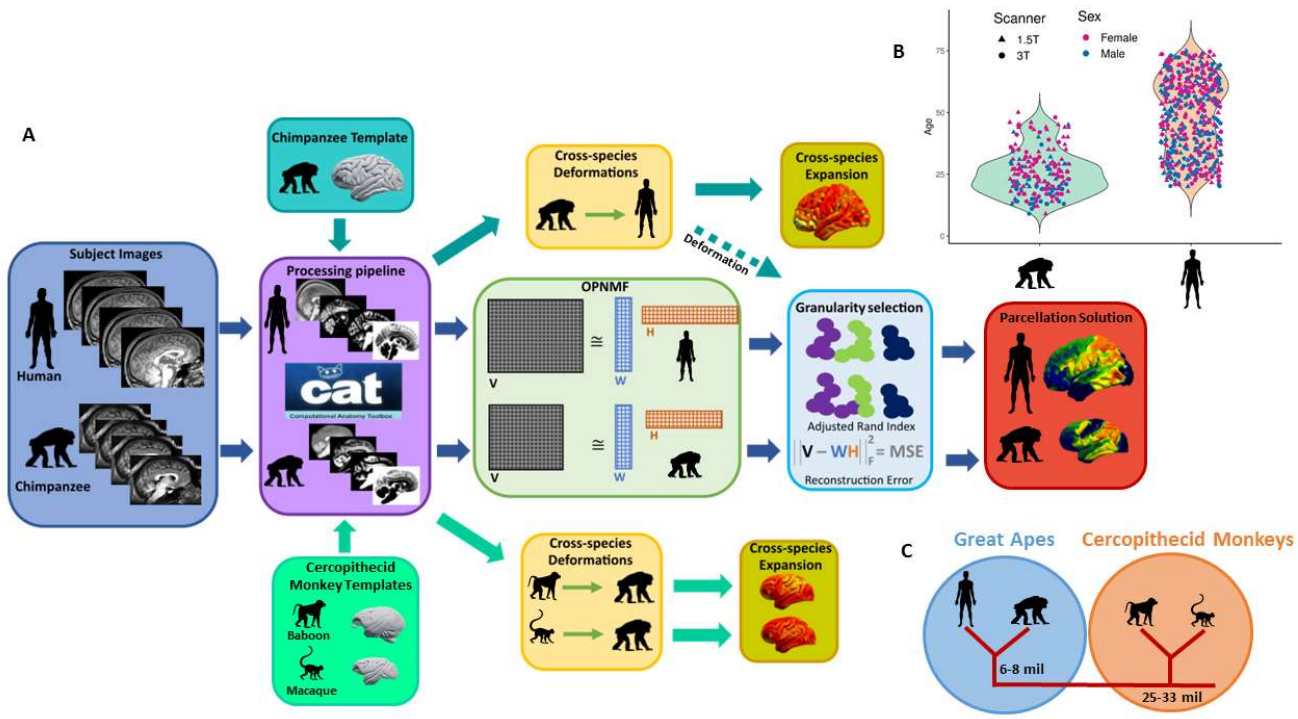

Figure 1. Overview of our comparative approach. A – Workflow outlining the steps taken in our comparative approach by utilizing OPNMF and creating cross-species expansion maps. B – The age, sex, and scanner field strength distribution of the chimpanzee (N=189) and human (N=480) samples used in creating the OPNMF solutions for cross-species comparison. C – Diagram showing the phylogenetic relationship of humans to the other three primate species investigated in this study.

Comparative Brain Parcellation

OPNMF takes the volumetric GM maps and creates parcels or clusters which contain voxels that co-vary with on another across the sample. This unsupervised technique behaves similar to clustering[38] and requires an a priori decision on the number of factors or parcels to represent the original data[25]. The decision for the most appropriate OPNMF granularity was determined via assessing cross-species spatial similarity and the development of OPNMF solutions accuracy at different granularities (Fig. 2A). Cross-species parcel similarity was determined using the cluster similarity measure ARI. Chimpanzee parcellations are transformed to the human template space using the chimpanzee to human deformation map. Quality control of the chimpanzee to human deformation map was conducted by visually inspecting the Davi130 chimpanzee macroanatomical labels[8] in the human template space (Supplementary Figure 1). The granularity with highest ARI

represents common cross-species organizational patterns of GM covariance[27]. The RE indicates how accurately the input data (GM maps) can be represented by the OPNMF factorization. By increasing the number of factors, or parcels, more information can be used to represent the GM data and RE naturally decreases. Although this development is non-linear and sample specific (Fig. 2A). A relative plateau means that increasing the granularity only marginally improves the parcellations representation of the GM data and therefore, will largely model noise. Consequently, the beginning of the plateau provides a good tradeoff between the solutions reconstruction accuracy and number of factors. Finally, to ensure the robustness of the RE development curve, a computationally intensive 100 bootstraps were computed for each OPNMF granularity in both species independently.

The highest cross-species spatial similarity was found for the 17-factor solution with an ARI of 0.23 (Fig. 2A). This is not a very high ARI, although it is along with 16 a clear local maximum and contains many parcels with relatively high ARI (> 0.4) (Fig. 2B). The robust RE development curve did not show a clear indication of a plateau for both species. Instead, a relevant number of parcels is present in the range of 15 – 21 in chimpanzees and 14 – 20 in humans. Therefore, the 17-factor solution met our criteria for both chimpanzees (Fig. 3A) and humans (Fig. 3B) to conduct our cross-species comparative investigation.

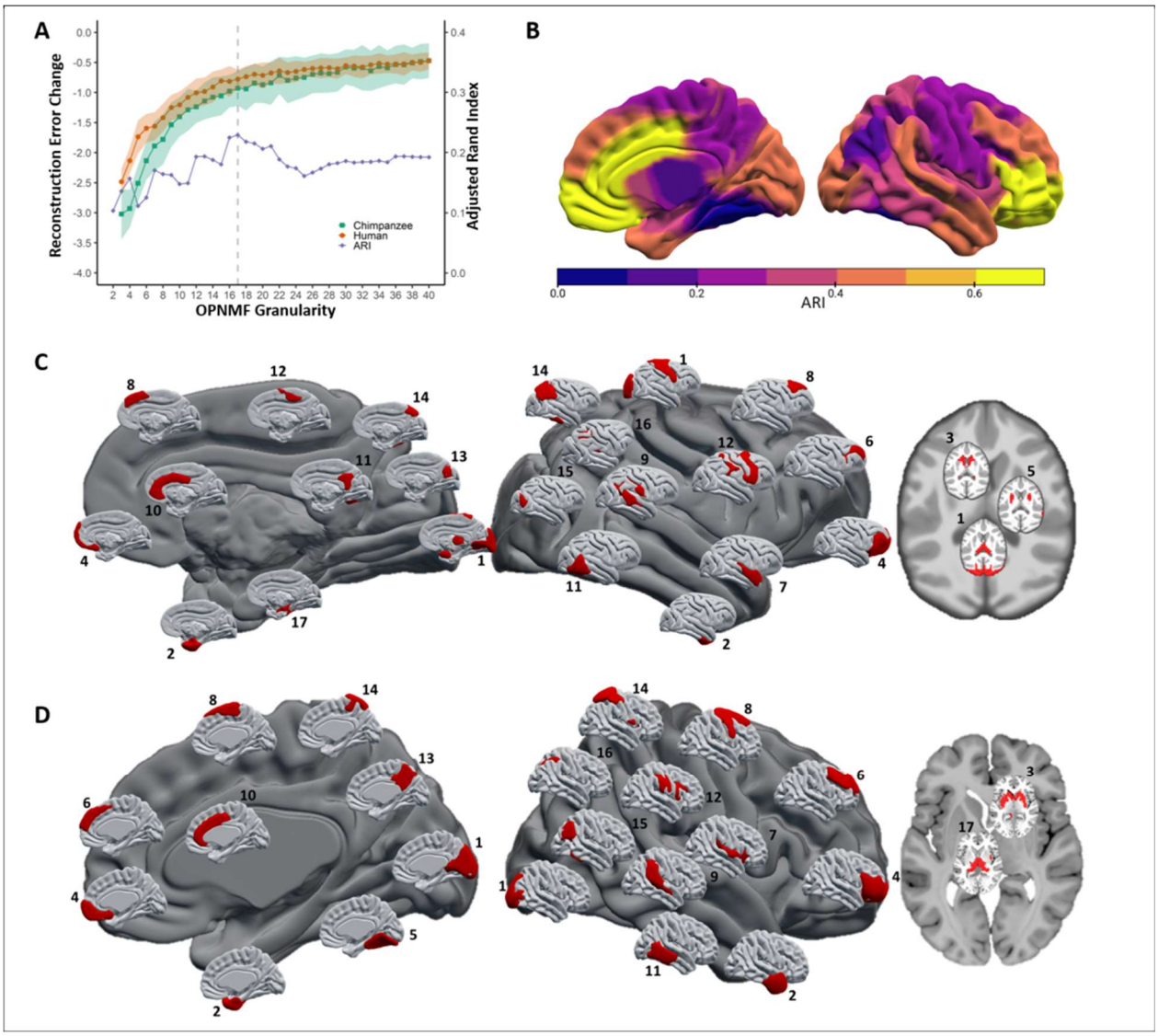

Figure 2 Selected OPNMF solution for cross-species comparison. A – OPNMF granularity selection utilizing ARI to assess cross-species similarity and change in reconstruction error (RE) over a granularity range of 2 – 40 factors and bootstrapped (k=100) to ensure stability. Cloud represents ±1 sd from the mean change in RE over 100 bootstraps and the gray dashed line represents the selected number of factors, 17. B – Presents the cross-species single factor ARI, whereby for each OPNMF factor the highest cross-species ARI is represented in human template space. C - Selected 17-factor OPNMF solution for chimpanzees. Macroanatomical labels are: 1 – occipital lobe, primary motor cortex, and thalamus, 2 – temporal pole, 3 – caudate nucleus, 4 – prefrontal and orbito-frontal cortex, 5 – putamen, 6 – middle frontal gyrus, 7 – superior temporal gyrus and anterior insula, 8 – posterior superior frontal gyrus, 9 – temporal parietal junction and supramarginal gyrus, 10 – anterior and middle cingulate cortex, 11 – posterior cingulate, precuneus, and peristriate cortex, 12 – supplementary and pre-motor areas, 13 – cuneus and medial occipital-parietal sulcus, 14 – superior and inferior parietal lobe and inferior temporal gyrus, 15 – lateral parietal-occipital sulcus, 16 – superior parietal sulcus and posterior insula, 17 – amygdala and hippocampus. D – Human selected 17-factor OPNMF solution. Macroanatomical labels are: 1 – occipital lobe, 2 – temporal pole, 3 – putamen, caudate nucleus, amygdala, and hippocampus, 4 – prefrontal and orbito-frontal cortex, 5 – lingual and fusiform gyrus, 6 – superior and middle frontal gyrus, 7 – insula, 8 – pre-central gyrus and pre-motor area, 9 – temporal parietal junction, 10 – anterior and middle cingulate cortex, 11 – posterior middle and inferior temporal gyri, 12 – supramarginal gyrus, inferior post-central gyrus, and inferior pre-central sulcus, 13 – precuneus, 14 – superior parietal lobe, 15 – angular and fusiform gyrus, 16 – superior parietal sulcus and parahippocampal cortex, 17 – thalamus.

The 17-factor OPNMF solutions in both chimpanzees (Fig. 2D) and humans (Fig. 2C) represents a data-driven parcellation of both species cerebral GM. These regions were established through a hard parcellation by assigning each voxel to the parcel with the highest weight, which is aided by the orthogonality constraint of OPNMF. Some resulting brain parcels closely align with known macroanatomical regions within both species. Both species 17-factor solutions contained parcels accurately representing the orbito-frontal cortex, middle frontal gyrus, anterior and middle cingulate cortex, and the temporal pole (Fig. 2C&D). In humans additionally parcels separated the insula, superior parietal lobule, precuneus, occipital lobe, and thalamus (Fig. 2D). On the other hand, chimpanzees additionally showed parcels that separated the pre-motor cortex, hippocampus, putamen, and caudate nucleus (Fig. 2C). The parcels representing the orbito-frontal cortex and the cingulate cortex show the highest cross-species similarity with an ARI of 0.66 and 0.64 respectively (Fig. 2B). This was assessed by calculating the highest single parcel-to-parcel cross-species similarity. A striking difference between the species can be seen in the parcellation of the sensory-motor cortices. In chimpanzees, two parcels represented major sensory-motor structures, one for the occipital lobe, pre- and post-central gyrus, and thalamus and another for the pre-motor cortex. In humans, separate parcels represented the thalamus and occipital lobe while the motor and pre-motor cortices are split between different parcels. Specifically in humans, multi-modal parietal regions like the precuneus, superior parietal lobule, angular gyrus, and temporal-parietal junction were more specifically parcellated compared to chimpanzees.

Comparison of Brain Aging and Relative Expansion between Chimpanzees and Humans

Age-mediated GM decline in chimpanzees and humans was assessed for the OPNMF 17-factor solution. The average GM density of each parcel was used as the dependent variable in a multiple linear regression model with age, sex, total intracranial volume (TIV), and scanner field strength as independent variables, as has been conducted previously[8]. To improve comparability, the human sample age range was matched to the chimpanzees by accounting for the interspecies differences in brain aging. The comparative aging difference of human years equal to 1.15 years in chimpanzees was used based on a comprehensive study using a combination of anatomic, genetic, and behavioral data[39]. Accordingly, as the oldest chimpanzees were 50 years old humans over 58

years old were removed to include 304 IXI subjects (150 females; mean age = 39.0±11.0) for the age regression model. Of note, this represents a middle-aged human sample, including minimal morphological changes due to age-related neurodegenerative or pre-clinical conditions such as mild cognitive impairment. In both species, significant age effects were found in nearly all parcels following correction for multiple comparisons across parcels at $p \leq 0.05$[40]. Humans showed aging effects across all parcels, largest in the frontal cortex and in particular, the PFC. Chimpanzees displayed overall aging effects in all parcels except for three, which represent the peristriate cortex, posterior insula, cuneus, and superior parietal sulcus. Both species showed a relatively low aging effect in occipital and motor areas. The largest aging effect in chimpanzees was found in the striatum, in particular the caudate nucleus. Humans showed overall a much greater age effect compared to chimpanzees. Additionally, a comparable aging effect and distribution was found when employing the higher granularity macroanatomical Davi130 parcellation[8] in chimpanzees and humans (Supplementary Figure 2).

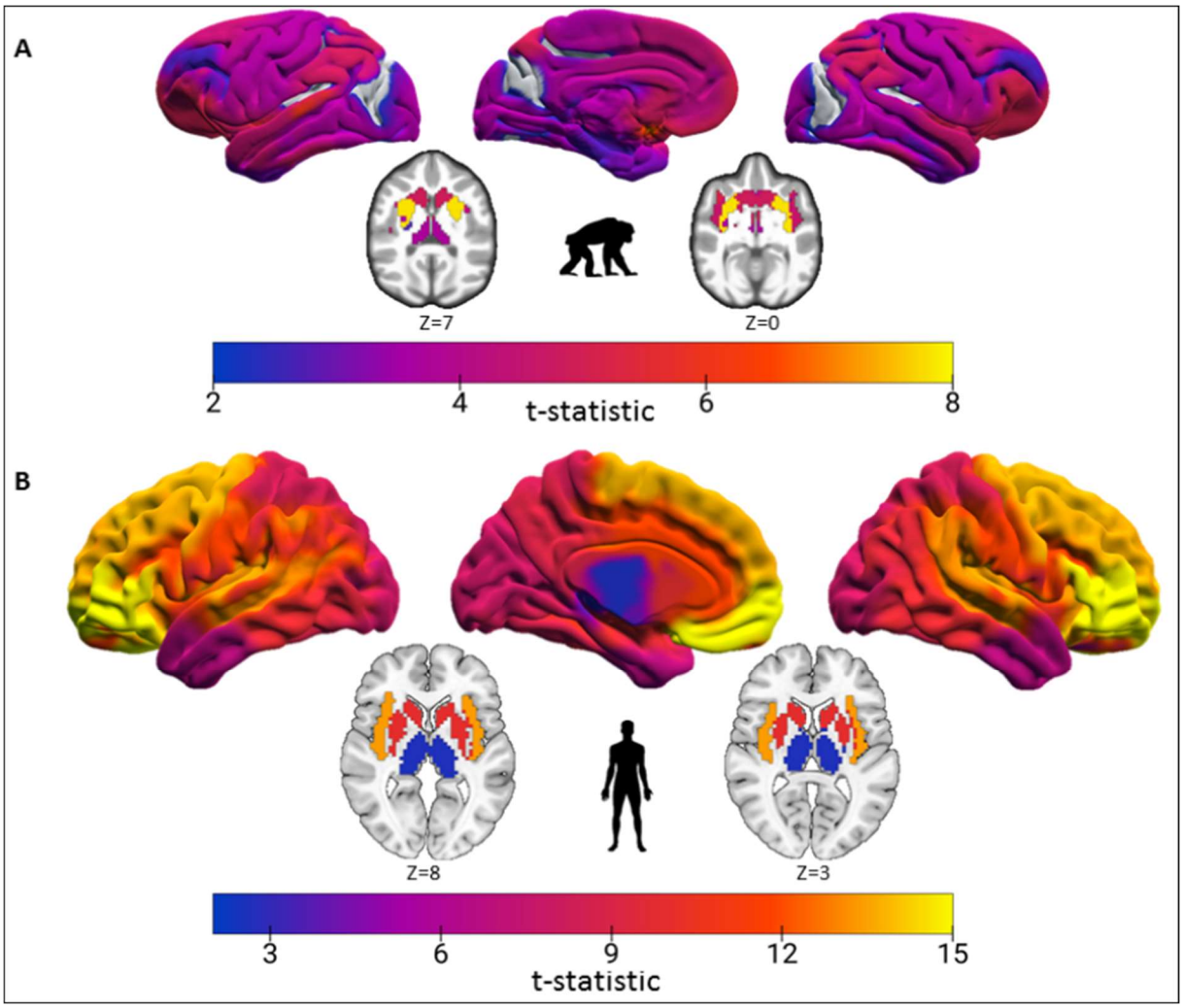

Figure 3. **Comparison of aging effect on GM volume**. OPNMF 17-factor solution age-mediated GM changes presented as factor-wise regression model absolute t-statistics in A - chimpanzees and B – humans. The t-statistic of significant parcels are plotted and determined by a FWE $p \leq 0.05$.

Utilizing the 17-factor solution, we compared the cross-species expansion based on population representative T1w templates from humans[33], chimpanzees[8], olive baboons[34] and rhesus

macaques[35–37]. Using template images provides the added benefit of artificially improved tissue contrast in addition to being representative of an average brain within a particular species aiding generalizability. Cross-species non-linear registrations were computed to provide estimations for the expansion from chimpanzee to human, baboon to chimpanzee, and macaque to chimpanzee.

In chimpanzee to human expansion, the largest deformation was found in the orbito-frontal cortex, which additionally showed the greatest aging effect (Fig. 3B) and highest cross-species parcel similarity (Fig. 2B). High expansion was additionally found in other multimodal association cortical areas such as the middle and medial frontal cortex, superior parietal, precuneus, insula, and cingulate cortex (Fig. 5A). The large expansion in frontal and parietal regions are comparable to those shown using cortical surface measures to estimate the expansion from chimpanzee to human[20] as well as macaque to human [24]. Low chimpanzee to human expansion was found in temporal, occipital, motor, and subcortical areas (Fig. 5A). When comparing the chimpanzee to human (Fig. 5A) with the baboon (Fig. 5B) and macaque (Fig. 5C) to chimpanzee expansion maps, similar low expansion was found in the temporal lobe and subcortical regions as well as relatively large deformations in the frontal and superior parietal lobe. The general pattern of expansion from the two cercopithecid monkeys to chimpanzees is similar although some regional differences are present. In baboon to chimpanzee, the largest expansion occurred in the superior frontal gyrus/pre-motor area (Fig. 5B) while in macaque to chimpanzee, the sulcal fundi of the parietal lobe and posterior insula (Fig. 5C) featured the largest expansion. Furthermore, macaque to chimpanzee showed comparably more expansion in the occipital-parietal junction and lower expansion in the motor/pre-motor area, occipital cortex, and basal ganglia compared to baboon to chimpanzee expansion. To summarize, chimpanzee to human as well as cercopithecid monkeys to chimpanzee expansion maps all show relatively high expansion in frontal and parietal cortical regions. Chimpanzee to human features the greatest expansion in prefrontal areas while in cercopithecid monkeys to chimpanzee the largest expansion was seen in pre-motor/frontal and lateral parietal regions. Finally, notable differences between macaques and baboons relative to chimpanzees are seen in the degree of expansion within unimodal and sensory motors areas.

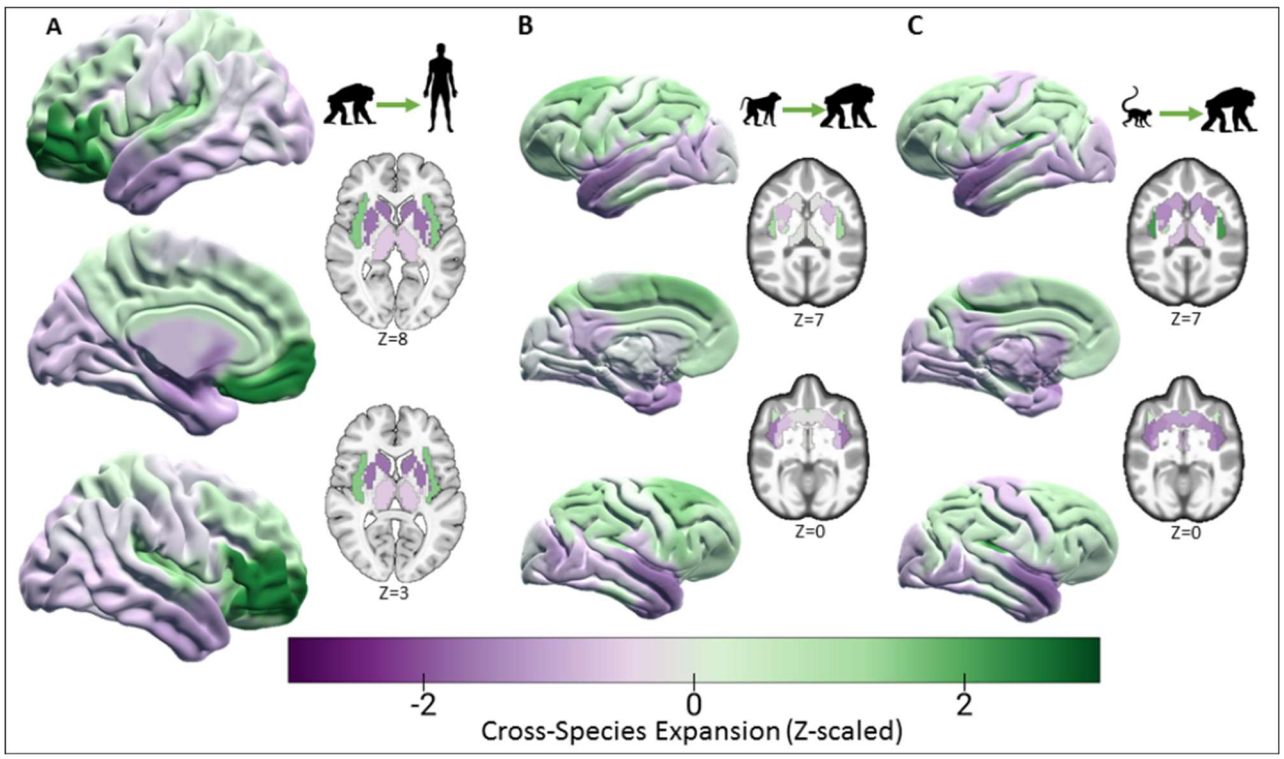

Figure 4. Cross-species expansion. OPNMF 17-factor solution volumetric Cross-species expansion in A - chimpanzee to human, B - baboon to chimpanzee, & C - macaque to chimpanzee. Expansion values have been z-scaled for easier comparison.

Correlation between Aging and Cross-species Expansion in Chimpanzees and Humans

We investigated the relationship between cross-species expansion (Fig. 4) and age-mediated GM changes (Fig. 3) in chimpanzees and humans. For humans, brain aging was compared with relative cortical expansion from chimpanzee to human (Fig. 5A) while for chimpanzees, aging effect was compared with both baboon and macaque (Fig. 5B). A strong positive correlation was found between cross-species expansion and the aging effect in humans (Fig. 5A), following permutation testing at $p \leq 0.05$ ($r = 0.59$; $p = 0.004$). This relationship is particularly evident in the orbito-frontal cortex and insula, which presents considerable expansion as well as an extensive aging effect. Relatively low aging effects and less cross-species expansion was found in the basal ganglia, occipital lobe, temporal pole, and medial temporal lobe. This general association was replicated in the lifespan eNKI (Enhanced Nathan Kline Institute; $n = 765$; $r = 0.51$; $p = 0.01$)[41] dataset using the same OPNMF parcellation to extract the aging effect (Supplementary Figure 4).

In chimpanzees, no significant relationship was seen between aging and baboon to chimpanzee cross-species expansion ($r = -0.005$, $p = 0.49$) although a marked negative correlation was found in macaque to chimpanzee expansion ($r = -0.53$, $p = 0.01$). Even though the macaque and baboon to chimpanzee expansion maps show a quite similar spatial distribution, there is an apparent trend that regions showing large chimpanzee age effect have low macaque to chimpanzee expansion and the opposite for regions with low aging effect. This is driven by the comparably lower macaque to chimpanzee expansion in the basal ganglia, which shows a large age effect in chimpanzees and the higher expansion in the peristriate cortex and the lateral parietal and posterior insula cortices that presents lower aging effects in chimpanzees.

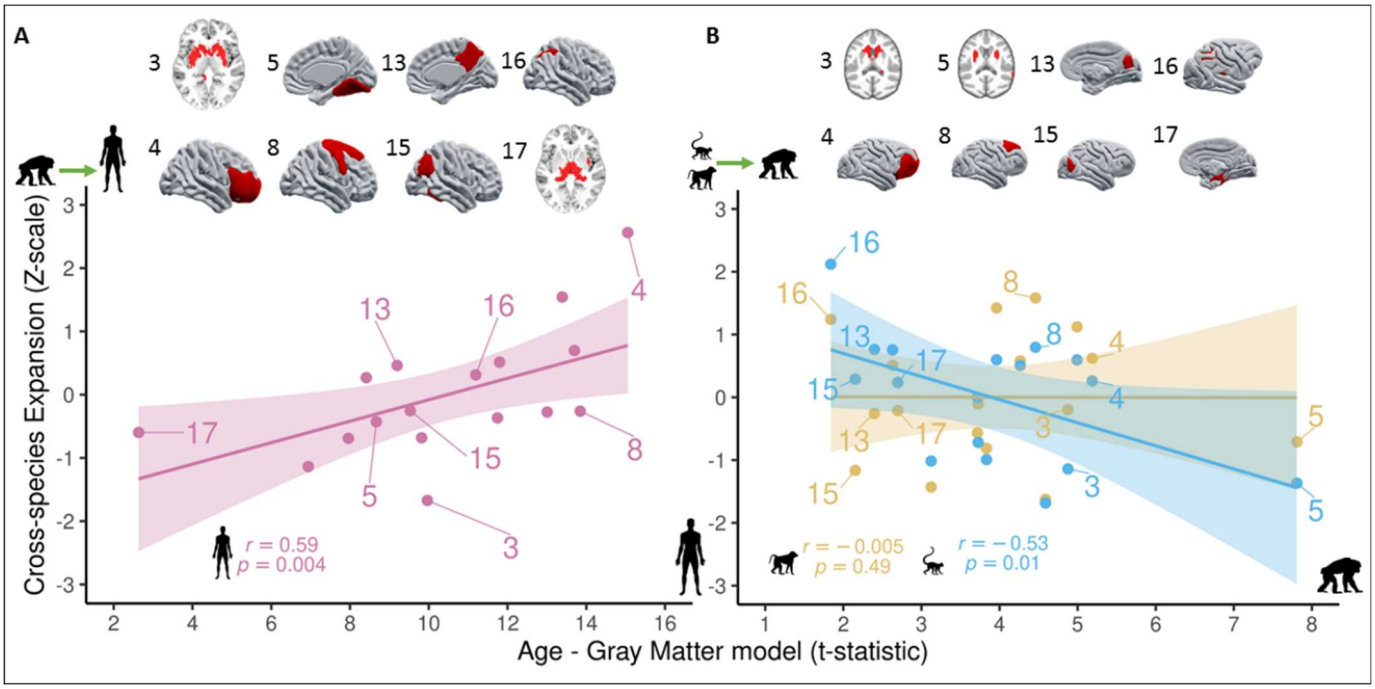

Figure 5. **Aging – expansion comparison.** Scatter plots showing of cross-species expansion and aging effect between A – chimpanzee to human expansion and human aging effect (Pink), B – macaque to chimpanzee

expansion and chimpanzee aging effect (Blue) and baboon to chimpanzee expansion and chimpanzee aging effect (Yellow). A selection of single OPNMF factors in both species are presented. Significance (p) of correlation (Person's r) for cross-species expansion and aging effect relationship is determined by permutation testing (k = 100 000).

Discussion

Through our comparative framework, we found a human-specific positive relationship between age-related GM decline and cortical expansion in comparison to chimpanzees. In chimpanzees, on the other hand, there was no correlation between the spatial distribution of aging effect and areas of cortical cross-species expansion relative to baboons and a positive correlation with the expansion relative to macaques. These findings suggest that the extensive expansion of higher-order cortical areas in human brain evolution, which is dominated by the PFC, and in particular the orbito-frontal cortex, comes at the price of more pronounced age-related deterioration.

We demonstrated OPNMFs ability to provide a low dimensional space matching macroanatomy that serves as a basis for cross-species comparison of brain organization. Our approach (Fig. 1A) is centered on OPNMF, which establishes a brain parcellation that contains species-specific information that also identifies comparable organizational features between species. The chimpanzee factorization solution (Fig. 2D) shows overall hemispheric symmetry, spatial contiguity, and aligns with known macroanatomical structures[8] which were reported in previous applications of OPNMF in humans[25,28–30,42]. The 17-factor solution that was selected based on cross-species similarity and within-species reconstruction accuracy comprises a very similar granularity that was selected in OPNMF for infants[42] and an adolescent human sample[30]. Along with the similar granularity, some human (Fig. 2C) and chimpanzee (Fig. 2D) parcels show apparent spatial similarity to previously reported OPNMF solutions[30,42]. Similarities include parcels representing the precuneus, insula, and superior parietal lobe, in the human factorization while both the chimpanzee and human solutions show similarities to previous findings in the PFC and temporal pole. Additionally, the superior parietal lobe and PFC parcels show similarities to spatial clusters representing genetic influence on cortical thickness[43].

The PFC plays an important role in higher-order cognitive functions, such as executive control[21,44] and working memory[45]. The OPNMF 17-factor solution created independently in chimpanzees (Fig. 2D) and humans (Fig. 2C) established a parcel representing the ventrolateral and orbital parts of the PFC. This region showed the highest cross-species similarity as well being expanded greatly in humans relative to chimpanzees. Therefore, the uniqueness of this region's GM organization was conserved between humans and chimpanzees, even though there was considerable cross-species expansion. Despite the PFC being proportionally larger in humans compared to chimpanzees [11], which is due in part to allometric scaling[46,47]. Our multivariate data-driven analysis suggests a possible similarity in the organization of the ventral and orbital sub-regions of the PFC. Furthermore, this region showed an exceptionally large GM aging effect in humans as well as a high degree of expansion in humans relative to chimpanzees. This suggests that the greater expansion of PFC, which has been instrumental in evolutionary changes in primate cognition[48], comes with the detriment of severe age-related GM decrease in humans. The much greater PFC expansion and aging effect in humans compared to chimpanzees, provides an additional dimension to the "last in, first out" hypothesis[23] of later developmental maturation and aging. With later evolutionary expansion also related to early and strong age-mediated GM morphology decline, furthering previous research showing similarities between macaque to human expansion and neurodevelopment[24].

The relationship between human GM volume decline and cortical expansion indicates an evolutionary link between functional development of these particular cortical areas in humans and increased vulnerability to neurodegenerative processes. Interestingly, such a relationship was not present in the expanded cortical regions of chimpanzee relative to baboons and macaques even though a significant GM decline was present in chimpanzees [8]. The main difference between humans and chimpanzees seems to be the more prominent expansion in sensorimotor regions in chimpanzees relative to the cercopithecid monkeys, whereas regions of human cortical expansion relative to chimpanzees is generally seen in more multimodal association regions. This could be related to chimpanzees improved abilities for tool use and spatial understanding as compared to cercopithecid monkeys although showing similar abilities in social-cognitive tasks[49].

In general, multimodal association cortex in humans show greater expansion as well as large aging effects on GM volume. Those multimodal cortical areas are characterized by lower neuronal cell density, as well as higher dendritic branching and spine numbers of pyramidal neurons[50,51]. Interestingly, compared to other great apes, the human brain has a large neuropil fraction in the frontal pole[52] and the anterior insula[53]. The neuropil fraction represents the space surrounding cell bodies occupied by dendritic and axonal interconnectedness through local intrinsic and extrinsic connections of a region. Both these areas (frontal pole and insula) show a combination of large expansion and aging effect on GM volume (Fig. 4A) in humans. With dendritic reduction and synapse loss being characteristics of normal aging processes[54], the relatively increased neuropil space of human association cortex may partly explain the aging – expansion relationship we observe.

Some possible neurobiological mechanisms could explain the large aging effect in regions that expanded most in humans relative to chimpanzees. The medial and orbito-frontal cortex as well as the insula that displayed large expansion and aging effects have been previously found to have high deterioration of glucose metabolism and large accumulation uptake of β-amyloid in human aging[55–57]. Additionally, the novel relationship we present may aid future research to better understand the neurobiological mechanism of why certain areas have expanded more than others.

Several considerations need to be considered when interpreting the results presented in this study. First, our voxel-based morphometry analysis was limited to structural information present in the T1w contrast and does not include structural connectivity or functional dynamics. Such complimentary information provided by additional modalities will help to establish a more comprehensive cross-species comparison. Second, our inferences of age-related GM volume decline are driven by cross-sectional normal aging data (age $\leq$ 58 y/o), although a longitudinal design can provide additional information on structural changes that occur to the brain throughout the lifespan. Third, to infer the unique relationship in human evolution between aging and regions of cortical expansion we only used templates of one great ape species (chimpanzee) and two different cercopithecid monkey species (macaque & baboon). Further research is required using additional primate species. A broader phylogenetic investigation will enable a better understanding at which evolutionary branches these aspects of the neurobiology of aging occur.

In conclusion, we demonstrate the applicability of a data-driven comparative framework in revealing organizational features of great ape brains. By establishing a species-specific parcellation containing both inter- and intra-species GM organizational features, we found a novel relationship of cortical expansion and age-related decline in great ape evolution. Our multivariate data-driven framework found regions with high expansion to show large age-mediated GM decline in humans, whereas this was not present in chimpanzees. These findings allude to a possible cost the human cortex pays, in the form of age-mediated GM decline, because of evolutionary expansion.

Methods

Sample Description

The chimpanzee T1w MRI scans were provided by the NCBR containing brain scans of 223 captive animals (137 females; 9 - 54 y/o; mean age 26.9 ± 10.2 years). The chimpanzees were housed at the National Center for Chimpanzee Care (NCC) at The University of Texas MD Cancer Center (N=147; 1.5 Tesla G.E echo-speed Horizon LX scanner) or the Yerkes National Primate Research Center (YNPRC; N=76; 3.0 Tesla Siemens Trio scanner). The MRI scanning procedures for chimpanzees at both the NCC and YNPRC were designed to minimize stress for the animals. Data were acquired with the approval of ethics committees at both sites and were obtained prior to the 2015 implementation of the U.S. Fish and Wildlife Service and National Institutes of Health regulations governing research with chimpanzees. Image quality control (QC) was conducted by assessing sample outliers in voxel-wise GM intensity correlations. 194 chimpanzees (130 females, 9 - 54 y/o, mean age = 26.2 ± 9.9) passed QC. To minimize the effect of extreme aging on the OPNMF solutions subjects over 50 years old were removed for a final sample of 189 chimpanzees (126 females, 9 - 50 y/o, mean age = 25.6 ± 9.1).

The human structural T1w MRI scans were provided from the IXI (Information eXtraction from Images) dataset. This open dataset was specifically chosen for comparison with the NCBR chimpanzees as it contains both 1.5 and 3 Tesla brain scans and has a comparable distribution of age and sex. IXI consists of 565 healthy subjects (314 females; 20 - 86 y/o; mean age 48.69 ± 16.46 years) without missing metadata. To further match the two NCBR scanners, subjects from the Hammersmith Hospital (HH; N=181; 3.0 Tesla Philips Medical Systems Intera scanner) and Guy's Hospital (GUYS; N=315; 1.5 Tesla Philips Medical Systems Gyroscan Intera scanner) were considered. These 496 subjects (270 females; 20 - 86 y/o; mean age 49.57 ± 16.28 years) all passed QC. To aid in comparability to the chimpanzee sample, the very old IXI subjects (>75 y/o) were removed for the construction of the OPNMF solutions for a final sample of 480 subjects (262 females, 20 - 74 y/o, mean age = 48.7 ± 16.5). We used the eNKI open neuroimaging dataset[41] to replicate the aging – expansion relationship in a larger lifespan sample. The eNKI scans were all acquired using a single 3T scanner (Siemens Magnetom TrioTim). T1w images were obtained using a MPRAGE sequence with 1mm isotropic voxels and TR = 1900 ms. The T1w images were preprocessed the same as IXI using CAT12. Following preprocessing, patient identified subjects were removed and QC was conducted by removing subjects that had CAT12 image quality ratings above two standard deviation from the mean. We then used 765 images from eNKI[41] (502 females; 6 – 85 y/o; mean age = 39.9 ± 22.2) for our replication analysis.

Image Processing

The chimpanzee (NCBR) and human (IXI, & eNKI) samples were preprocessed using the SPM12 (Statistical Parametric Mapping; https://www.fil.ion.ucl.ac.uk/spm/software/spm12/; v7487) toolbox, CAT12[58] (Computational Anatomy Toolbox; http://www.neuro.uni-jena.de/cat/; r1725). The NCBR sample was processed utilizing the newly established chimpanzee specific pipeline[8] while the IXI sample utilized the default human processing pipeline with high accuracy shooting regestration[59]. The general steps of preprocessing were, first, the single subject images are affine registered to template space and segmented into the three tissue types, gray matter, white matter, and cerebrospinal fluid, utilizing a tissue probability map (TPM). Next, each tissue map is nonlinearly

registered to five shooting templates with increasing registration accuracy[59] to bring all subjects' tissue maps into the same template space. Finally, the deformation fields required to register the subjects into template space are used to modulate the tissue maps to conserve original local volume. Following preprocessing the modulated GM maps for each species were down-sampled (2 mm & 3 mm resolution) and smoothed (4 mm & 6 mm full width half maximum) in the NCBR and IXI samples, respectively. Finally, a GM mask at 0.3 and 0.2 probability for the chimpanzee and human samples respectively was applied encompassing the cortex and basal ganglia.

Orthogonal Projective Non-negative Matrix Factorization (OPNMF) and Granularity Selection

To estimate the GM structural covariance parcellation the orthogonal variant of NMF[60], OPNMF was used[225,26]. OPNMF establishes a low dimensional representation of the voxel-wise GM data where non-negativity is enforced on all elements. The low dimensional space comprises a parcellation matrix with the factorization loadings for each voxel and a subject matrix containing the subject loadings for each component. By constraining the matrices to non-negative values provides a parts-based representation of the cerebral GM data by the way of spatially continuous and additive covariance parcels. A hard parcellation is created by appointing each voxel to the parcel with the highest weight. Selection of the most appropriate OPNMF granularity for cross-species comparison was assessed through analysis of the reconstruction error development over bootstraps (k = 100) in combination with cross-species OPNMF solution parcel similarity over the range of 2 – 40 parcels. Further details can be found in the Supplementary.

Template Processing and Expansion Maps

Employing CAT12 preprocessing we established cross-species deformation maps which represent an approximation of the cross-species expansion. Utilizing population average T1 maps of a species and the processing pipeline of the target species, we could create deformation maps that represent an estimation of cross-species expansion. Species templates were selected as they represent an average brain, improving interpretability of the expansion estimates as well as having high tissue contrasts aiding segmentation and registration. We used two species-specific processing pipeline, chimpanzee [8] and human, to create our expansion maps. The chimpanzee to human expansion map was created using the chimpanzee template in the human pipeline while the baboon and macaque to chimpanzee expansion maps were created using the chimpanzee pipeline[8] with the baboon[34] and macaque[35–37] templates respectively. We averaged the expansion map of three commonly used macaque templates to encompass inter-sample variation. Further information regarding the expansion map creation can be found in the Supplementary. QC was performed on all deformation and expansion maps by assessing the smoothness and feasibility of the macroanatomical structures. Additionally, for the chimpanzee to human map we visually inspected the spatial location of the Davi130[8] regions when registered to the human template space (Supplementary Figure 1).

Gray Matter Aging and Expansion Analyses

We assessed the relationship between age related GM decline and relative expansion in chimpanzees and humans, utilizing the data-driven low dimensional OPNMF solution. The aging effect on GM volume was assessed for the chimpanzee and human samples utilizing an OPNMF

473 parcel-wise linear regression model. The age-range of the IXI sample was matched to the chimpanzee
474 to improve comparability, by accounting for the difference in aging processes (human ≈ 1.15x
475 chimpanzee)[39]. Therefore, 304 IXI subjects (females = 150; 20 – 58 y/o; age = 39.0 ± 11.0) and 189
476 chimpanzees (126 females; 9 - 50 y/o; age = 25.6 ± 9.1) were used for the age regression model.
477 Average GM density values for each OPNMF parcel from the chimpanzees and humans were entered
478 into a regression model for each species, as the independent variable with age, sex, total intracranial
479 volume (TIV), and scanner field strength as the dependent variables. Parcels showing a significant age
480 effect was assessed at $p \leq 0.05$ following correction for multiple comparisons using FWE[40]. The parcel-
481 wise age model t-statistics in the human sample were compared with the chimpanzee to human
482 expansion while the chimpanzee age effect was compared with the baboon and macaque cross-
483 species expansion. Cross-species expansion was estimated by taking the mean expansion from each
484 component for the various cross-species expansion maps and z-scored to present the inter-regional
485 inter-species expansion. Significance of Pearson's correlation and difference between correlations
486 was determined through permutation testing (k=100 000) at $p \leq 0.05$. Finally, the human parcel-wise
487 age effect was replicated in the eNKI[41] lifespan neuroimaging dataset and correlated with
488 chimpanzee to human expansion to assess the robustness of our findings in humans.

489 **Data and Code Availability**

490 The chimpanzee (www.chimpanzeebrain.org) and two human neuroimaging datasets, IXI
491 (http://brain-development.org/ixi-dataset/) and eNKI
492 (http://fcon_1000.projects.nitrc.org/indi/enhanced/index.html) are openly available. The human
493 (MNI) and chimpanzee (JunaChimp) reference templates are available as part of the CAT12 (v12.7+)
494 toolbox or can be individually downloaded at
495 http://www.bic.mni.mcgill.ca/ServicesAtlases/ICBM152NLin2009 and http://junachimp.inm7.de/
496 respectively. The cercopithecid monkey template are also openly available for download, baboon
497 (Haiko89 - https://www.nitrc.org/projects/haiko89/) and macaques (D99 –
498 https://afni.nimh.nih.gov/pub/dist/doc/htmldoc/nonhuman/macaque_tempatl/atlas_d99v2.html;
499 INIA19 – https://www.nitrc.org/projects/inia19/; NMT -
500 https://afni.nimh.nih.gov/pub/dist/doc/htmldoc/nonhuman/macaque_tempatl/template_nmtv2.ht
501 ml#download-symmetric-nmt-v2-datasets). The GM masks for chimpanzees and humans can be
502 downloaded at https://zenodo.org/record/6463123#.YyljX_exVhG. The remaining data created for
503 this manuscript can be downloaded at https://zenodo.org/record/7116203#.YzLvCfexWV4 and code
504 for the analyses can be found at https://github.com/viko18/GreatApe_Aging.

505 # References

1. Crivello, F., Tzourio-Mazoyer, N., Tzourio, C. & Mazoyer, B. Longitudinal assessment of global and regional rate of grey matter atrophy in 1,172 healthy older adults: Modulation by sex and age. *PLoS ONE* **9**, (2014).
2. Good, C. D. *et al.* A voxel-based morphometric study of ageing in 465 normal adult human brains. *Neuroimage* **14**, 21–36 (2001).
3. Minkova, L. *et al.* Gray matter asymmetries in aging and neurodegeneration: A review and meta-analysis. *Human Brain Mapping* **38**, 5890–5904 (2017).

4. Vogt, C. & Vogt, O. Die vergleichend-architektonische und die vergleichend-reizphysiologische Felderung der Großhirnrinde unter besonderer Berücksichtigung der menschlichen. *Naturwissenschaften* **14**, 1190–1194 (1926).
5. Milham, M. P. *et al.* An Open Resource for Non-human Primate Imaging. *Neuron* **100**, (2018).
6. Friedrich, P. *et al.* Imaging evolution of the primate brain: the next frontier? *Neuroimage* **228**, 117685 (2021).
7. Mulholland, M. M., Sherwood, C. C., Schapiro, S. J., Raghanti, M. A. & Hopkins, W. D. Age- and cognition-related differences in the gray matter volume of the chimpanzee brain (Pan troglodytes): A voxel-based morphometry and conjunction analysis. *American Journal of Primatology* **83**, e23264 (2021).
8. Vickery, S. *et al.* Chimpanzee brain morphometry utilizing standardized MRI preprocessing and macroanatomical annotations. *eLife* **9**, e60136 (2020).
9. Sherwood, C. C. *et al.* Aging of the cerebral cortex differs between humans and chimpanzees. *Proc Natl Acad Sci U S A* **108**, 13029–13034 (2011).
10. Hopkins, W. D. *et al.* Age-related changes in chimpanzee (Pan troglodytes) cognition: Cross-sectional and longitudinal analyses. *American Journal of Primatology* **83**, e23214 (2021).
11. Donahue, C. J., Glasser, M. F., Preuss, T. M., Rilling, J. K. & Van Essen, D. C. Quantitative assessment of prefrontal cortex in humans relative to nonhuman primates. *Proceedings of the National Academy of Sciences* (2018).
12. Hopkins, W. D. & Nir, T. M. Planum temporale surface area and grey matter asymmetries in chimpanzees (Pan troglodytes): The effect of handedness and comparison with findings in humans. *Behavioural Brain Research* **208**, 436–443 (2010).
13. Schenker, N. M. *et al.* Broca's Area Homologue in Chimpanzees (Pan troglodytes): Probabilistic Mapping, Asymmetry, and Comparison to Humans. *Cereb Cortex* **20**, 730–742 (2010).
14. Langergraber, K. E. *et al.* Generation times in wild chimpanzees and gorillas suggest earlier divergence times in great ape and human evolution. *Proceedings of the National Academy of Sciences of the United States of America* **109**, 15716–15721 (2012).
15. Waterson, R. H., Lander, E. S. & Wilson, R. K. Initial sequence of the chimpanzee genome and comparison with the human genome. *Nature* **437**, 69–87 (2005).

16. Hopkins, W. D., Li, X., Crow, T. & Roberts, N. Vertex- and atlas-based comparisons in measures of cortical thickness, gyrification and white matter volume between humans and chimpanzees. *Brain Struct Funct* **222**, 229–245 (2017).
17. Hopkins, W. D. *et al.* Evolution of the central sulcus morphology in primates. **84**, 19–30 (2014).
18. Rilling, J. K. & Insel, T. R. The primate neocortex in comparative perspective using magnetic resonance imaging. *J Hum Evol* **37**, 191–223 (1999).
19. Bruner, E., Preuss, T. M., Chen, X. & Rilling, J. K. Evidence for expansion of the precuneus in human evolution. *Brain Struct Funct* **222**, 1053–1060 (2017).
20. Wei, Y. *et al.* Genetic mapping and evolutionary analysis of human-expanded cognitive networks. *Nat Commun* **10**, 4839 (2019).
21. Miller, E. K. The prefontral cortex and cognitive control. *Nat Rev Neurosci* **1**, 59–65 (2000).
22. Cavanna, A. E. & Trimble, M. R. The precuneus: a review of its functional anatomy and behavioural correlates. *Brain* **129**, 564–583 (2006).
23. Fjell, A. M., McEvoy, L., Holland, D., Dale, A. M. & Walhovd, K. B. What is normal in normal aging? Effects of aging, amyloid and Alzheimer's disease on the cerebral cortex and the hippocampus. *Progress in Neurobiology* **117**, 20–40 (2014).
24. Hill, J. *et al.* Similar patterns of cortical expansion during human development and evolution. *PNAS* **107**, 13135–13140 (2010).
25. Sotiras, A., Resnick, S. M. & Davatzikos, C. Finding imaging patterns of structural covariance via Non-Negative Matrix Factorization. *Neuroimage* **108**, 1–16 (2015).
26. Yang, Z. & Oja, E. Linear and Nonlinear Projective Nonnegative Matrix Factorization. *IEEE Transactions on Neural Networks* **21**, 734–749 (2010).
27. Alexander-Bloch, A., Giedd, J. N. & Bullmore, E. Imaging structural co-variance between human brain regions. *Nat Rev Neurosci* **14**, 322–336 (2013).
28. Nassar, R. *et al.* Gestational Age is Dimensionally Associated with Structural Brain Network Abnormalities Across Development. *Cereb Cortex* **29**, 2102–2114 (2019).
29. Patel, R. *et al.* Investigating microstructural variation in the human hippocampus using non-negative matrix factorization. *NeuroImage* **207**, 116348–116348 (2020).

30. Sotiras, A. *et al.* Patterns of coordinated cortical remodeling during adolescence and their associations with functional specialization and evolutionary expansion. *Proc Natl Acad Sci U S A* **114**, 3527–3532 (2017).
31. Varikuti, D. P. *et al.* Evaluation of non-negative matrix factorization of grey matter in age prediction. *Neuroimage* **173**, 394–410 (2018).
32. Gaser, C. *et al.* CAT – A Computational Anatomy Toolbox for the Analysis of Structural MRI Data. 2022.06.11.495736 Preprint at https://doi.org/10.1101/2022.06.11.495736 (2022).
33. Fonov, V. *et al.* Unbiased average age-appropriate atlases for pediatric studies. *NeuroImage* **54**, 313–327 (2011).
34. Love, S. A. *et al.* The average baboon brain: MRI templates and tissue probability maps from 89 individuals. *NeuroImage* **132**, 526–533 (2016).
35. Reveley, C. *et al.* Three-dimensional digital template atlas of the macaque brain. *Cerebral Cortex* (2017) doi:10.1093/cercor/bhw248.
36. Rohlfing, T. *et al.* The INIA19 Template and NeuroMaps Atlas for Primate Brain Image Parcellation and Spatial Normalization. *Frontiers in Neuroinformatics* **6**, 27–27 (2012).
37. Seidlitz, J. *et al.* A population MRI brain template and analysis tools for the macaque. *NeuroImage* **170**, 121–131 (2018).
38. Ding, C., He, X. & Simon, H. D. On the Equivalence of Nonnegative Matrix Factorization and Spectral Clustering. in *Proceedings of the 2005 SIAM International Conference on Data Mining (SDM)* 606–610 (Society for Industrial and Applied Mathematics, 2005). doi:10.1137/1.9781611972757.70.
39. Charvet, C. J. Cutting across structural and transcriptomic scales translates time across the lifespan in humans and chimpanzees. *Proceedings of the Royal Society B: Biological Sciences* **288**, 20202987 (2021).
40. Holm, S. A Simple Sequentially Rejective Multiple Test Procedure. *Scandinavian Journal of Statistics* **6**, 65–70 (1979).
41. Nooner, K. B. *et al.* The NKI-Rockland Sample: A Model for Accelerating the Pace of Discovery Science in Psychiatry. *Front Neurosci* **6**, 152 (2012).

42. Wang, F. *et al.* Developmental topography of cortical thickness during infancy. *PNAS* **116**, 15855–15860 (2019).
43. Chen, C.-H. *et al.* Genetic topography of brain morphology. *PNAS* **110**, 17089–17094 (2013).
44. Friedman, N. P. & Robbins, T. W. The role of prefrontal cortex in cognitive control and executive function. *Neuropsychopharmacol.* **47**, 72–89 (2022).
45. Owen, A. M., McMillan, K. M., Laird, A. R. & Bullmore, E. N-back working memory paradigm: a meta-analysis of normative functional neuroimaging studies. *Hum Brain Mapp* **25**, 46–59 (2005).
46. Barton, R. A. & Venditti, C. Human frontal lobes are not relatively large. *Proc Natl Acad Sci U S A* **110**, 9001–9006 (2013).
47. Smaers, J. B., Gómez-Robles, A., Parks, A. N. & Sherwood, C. C. Exceptional Evolutionary Expansion of Prefrontal Cortex in Great Apes and Humans. *Current Biology* **27**, 1549 (2017).
48. Preuss, T. M. & Wise, S. P. Evolution of prefrontal cortex. *Neuropsychopharmacol.* **47**, 3–19 (2022).
49. Schmitt, V., Pankau, B. & Fischer, J. Old World Monkeys Compare to Apes in the Primate Cognition Test Battery. *PLOS ONE* **7**, e32024 (2012).
50. Jacobs, B. *et al.* Regional dendritic and spine variation in human cerebral cortex: a quantitative golgi study. *Cereb Cortex* **11**, 558–571 (2001).
51. Sherwood, C. C. *et al.* Invariant Synapse Density and Neuronal Connectivity Scaling in Primate Neocortical Evolution. *Cerebral Cortex* **30**, 5604–5615 (2020).
52. Semendeferi, K. *et al.* Spatial organization of neurons in the frontal pole sets humans apart from great apes. *Cereb Cortex* **21**, 1485–1497 (2011).
53. Spocter, M. A. *et al.* Neuropil distribution in the cerebral cortex differs between humans and chimpanzees. *J Comp Neurol* **520**, 2917–2929 (2012).
54. Morrison, J. H. & Hof, P. R. Life and Death of Neurons in The Aging Cerebral Cortex. in *International Review of Neurobiology* vol. 81 41–57 (Academic Press, 2007).
55. Carbonell, F., Zijdenbos, A. P. & Bedell, B. J. Spatially Distributed Amyloid-β Reduces Glucose Metabolism in Mild Cognitive Impairment. *J Alzheimers Dis* **73**, 543–557 (2020).
56. Kakimoto, A. *et al.* Age-Related Sex-Specific Changes in Brain Metabolism and Morphology. *Journal of Nuclear Medicine* **57**, 221–225 (2016).

57. Lowe, A. J. *et al.* Targeting age-related differences in brain and cognition with multimodal imaging and connectome topography profiling. *Human Brain Mapping* **40**, 5213–5230 (2019).
58. Gaser, C., Dahnke, R., Kurth, K., Luders, E., & Alzheimer's Disease Neuroimaging Initiative. A computational Anatomy Toolbox for the Analysis of Structural MRI Data. *Neuroimage* (2020).
59. Ashburner, J. & Friston, K. J. Diffeomorphic registration using geodesic shooting and Gauss-Newton optimisation. *Neuroimage* **55**, 954–967 (2011).
60. Lee, D. D. & Seung, H. S. Learning the parts of objects by non-negative matrix factorization. *Nature* **401**, 788–791 (1999).oi.org/10.1038/nrn3465